

Phosphoantigens Glue Butyrophilin 3A1 and 2A1 to Activate V γ 9V δ 2 T Cells

The molecular basis for antigen recognition by $\gamma\delta$ T cells is unclear. Here, it shows how phosphoantigen (pAg) molecules function as “molecular glues” and then activate $\gamma\delta$ T cells.

Our understanding of antigen recognition by $\alpha\beta$ T cells has expanded greatly over the past 40 years. However, the molecular basis for antigen recognition by $\gamma\delta$ T cells remains elusive. V γ 9V δ 2 T cells—a major subtype of human circulating $\gamma\delta$ T cells—respond to multiple cancers and infectious diseases; they are specifically activated by small, non-peptidic diphosphate metabolites called pAgs. Later studies identified that sensing of pAgs in target cells requires butyrophilin 3A1 (BTN3A1). Crystallography has revealed that (*E*)-1-hydroxy-2-methyl-but-2-enyl 4-diphosphate (HMBPP), a very strong pAg of biological origin, binds to the BTN3A1’s intracellular B30.2 domain (BTN3A1 B30.2).¹ This intracellular binding triggers an extracellular conformational change that allows target cells to be recognized by $\gamma\delta$ T cells in a process referred to as inside-out signaling.¹ The earlier studies indicated that a BTN3A1 monomer alone is unlikely to trigger the pAg-induced extracellular conformational change. In 2020, butyrophilin 2A1 (BTN2A1) was shown to be a direct V γ 9 TCR ligand and induce activation of $\gamma\delta$ T cells with BTN3A1.²

To elucidate the structural basis for events inside and outside of cells and explore the molecular mechanism of signal transduction from the inside out, a research team led by Rey-Ting Guo (Hubei University, China) solved the apo-structure of BTN2A1 B30.2, as well as the structure of the BTN3A1 B30.2–HMBPP–BTN2A1 B30.2 complex.³ X-ray diffraction data were collected at **TLS 15A1** and **TPS 05A** of the NSRRC. The crystal structure of BTN2A1 B30.2 was found to adopt the characteristic B30.2 fold comprising a β -sandwich formed by two sets of antiparallel β sheets (sheets A and B) for its SPRY domain (**Fig. 1(a)**, see next page). The structure of the BTN2A1 B30.2 domain closely resembles that of the BTN3A1 B30.2 domain. However, a notable difference is the presence of a basic pocket on the surface of the BTN3A1 B30.2 domain, which has previously been implicated in HMBPP binding. By contrast, no such basic pocket is evident in the corresponding region in the BTN2A1 B30.2 structure (**Fig. 1(a)**), explaining BTN2A1’s inability to bind to HMBPP. Thereafter, we solved the structure of the BTN3A1 B30.2–HMBPP–BTN2A1 B30.2 complex (**Fig. 1(b)**). We found two BTN2A1 B30.2 molecules and two HMBPP-bound BTN3A1 B30.2

molecules in one asymmetric unit. The two BTN2A1 B30.2 polypeptides constitute a homodimer, and BTN3A1 engagement with HMBPP forms a composite interface for direct binding to BTN2A1, with HMBPP positioned at the center of the interface (**Fig. 1(b)**). The P α phosphate of HMBPP forms interactions with two residues of BTN2A1 (**Figs. 1(b): (i)**): one hydrogen bond and one salt bridge with Arg477 (BTN2A1, B chain) and one hydrogen bond with the main-chain N atom of Val511 (BTN2A1, A chain). The P β phosphate forms a hydrogen bond with Thr510 (BTN2A1, A chain). Several polar interactions were also identified at the interfaces of the BTN3A1 monomers and the BTN2A1 homodimer, including salt bridges and hydrogen bonds (**Figs. 1(b): (ii) and (iii)**).

Next, the team mutated the BTN2A1 residues that directly interact with HMBPP: Arg477, Thr510, and Val511 residues. In contrast to wild-type (WT) BTN2A1, none of these mutants caused V γ 9V δ 2 T-cell activation in the presence of HMBPP (**Figs. 2(a) and 2(b)**, see next page). Furthermore, the team generated a BTN2A1 double mutant (D455G/E457R) to disrupt the interaction of Asp455 and Glu457 with BTN3A1’s Trp350 and Trp391 residues and found that these mutations significantly reduced the extent of HMBPP-triggered V γ 9V δ 2 T-cell activation (**Figs. 2(a) and 2(b)**). These findings indicate that HMBPP is required as the “glue” for $\gamma\delta$ T-cell activation.

Previous studies that sought to explain the efficient immunosurveillance of V γ 9V δ 2 T cells have faced challenges due to the disparity between the binding affinity of BTN3A1 (in the micromolar range) and the potent cell activity of the exogenous pAg HMBPP (in the picomolar range). Here, the team found intracellular interactions between BTN2A1 and BTN3A1 as the basis for effective pAg sensing and inside-out signaling, which ultimately triggers $\gamma\delta$ T-cell responses. The complex formed by BTN3A1 and pAg acts as a composite interface, establishing direct binding with BTN2A1. This binding is facilitated by the presence of the pAg molecule at the center of the interface, effectively bridging the interaction. Therefore, the pAg acts as a molecular glue to form the BTN3A1–BTN2A1 complex, enabling efficient immunosurveillance by V γ 9V δ 2 T cells. (Reported by Rey-Ting Guo, Hubei University, China)

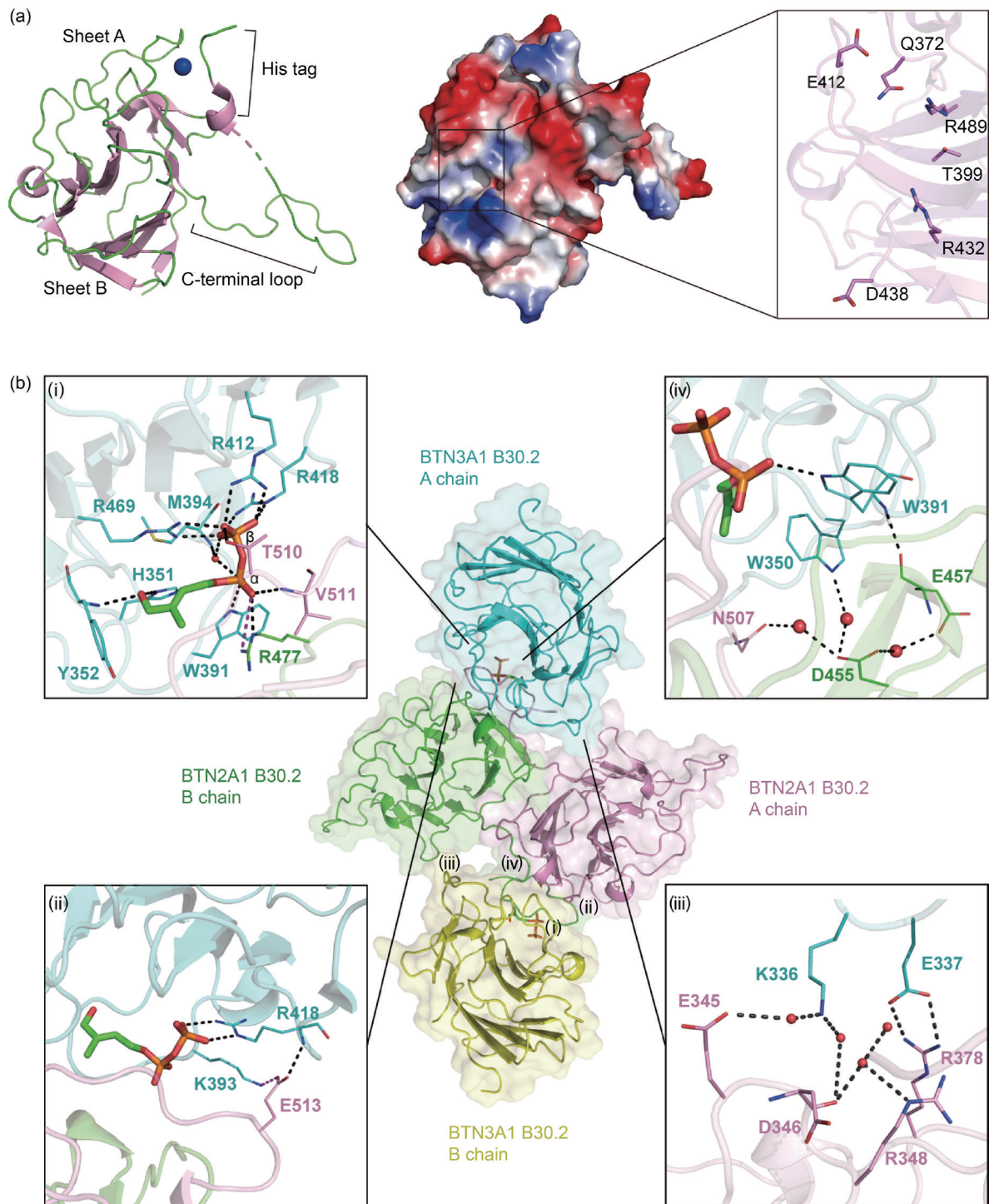


Fig. 1: The structures of the BTN2A1 B30.2 and BTN3A1 B30.2-HMBPP-BTN2A1 B30.2 complex. (a) Cartoon model of the apo BTN2A1 B30.2 crystal structure (left), electrostatic surface, and residues in the BTN2A1 B30.2 structure corresponding to BTN3A1 B30.2 (right). (b) The structure of the BTN3A1 B30.2-HMBPP-BTN2A1 B30.2 complex. Middle, cartoon representation of two BTN3A1 B30.2-HMBPP molecules (cyan and yellow) in complex with a BTN2A1 B30.2 homodimer (the A and B chains are shown in pink and green, respectively). Magnified views of the interactions between the BTN2A1 B30.2 dimer and the HMBPP-BTN3A1 B30.2 A chain are shown: HMBPP and the BTN2A1 and BTN3A1 B30.2 domains (i), BTN2A1 B30.2 and BTN3A1 B30.2 domains (ii, iii), and Trp350/Trp391 of BTN3A1 B30.2 and the BTN2A1 B30.2 domain (iv). Water molecules are shown as small red spheres. The black dashed lines indicate hydrogen bonds, and the purple dashed lines indicate salt bridges. [Reproduced from Ref. 3]

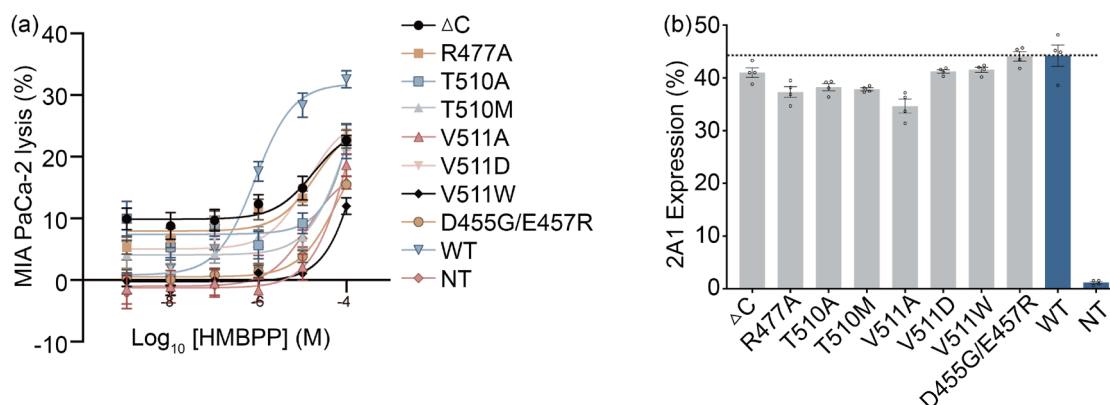


Fig. 2: Features of BTN2A1 B30.2 required for its association with BTN3A1 and for HMBPP-induced V γ 9V δ 2 T-cell activation. (a) Cytotoxicity of V γ 9V δ 2 T cells toward BTN2A1^{-/-} MIA PaCa-2 (2A1/2A2 KO, n=5, representative of two independent experiments) transfected with plasmids for the indicated 2A1 mutant variants pretreated with HMBPP (1 nM–100 μ M) overnight. Note that the 2A1 Δ C mutant was BTN2A1 with a truncated tail (truncated residues include LTGANGVTPEEGLTLHRVSLLE). Error bars: SEM. (b) Flow cytometry analysis of His-tagged 2A1 mutant variants in BTN2A1^{-/-} 293T cells (n=4, representative of two independent experiments), as detected by anti-His mAb. Error bars: SEM. [Reproduced from Ref. 3]

This report features the work of Rey-Ting Guo and his collaborators published in *Nature* **621**, 840 (2023).

TPS 05A Protein Microcrystallography

TLS 15A1 Biopharmaceuticals Protein Crystallography

- Protein Crystallography
- Biological Macromolecules, Protein Structures, Life Science

References

1. Y. Yang, L. Li, L. Yuan, X. Zhou, J. Duan, H. Xiao, N. Cai, S. Han, X. Ma, W. Liu, C.-C. Chen, L. Wang, X. Li, J. Chen, N. Kang, J. Chen, Z. Shen, S. R. Malwal, W. Liu, Y. Shi, E. Oldfield, R.-T. Guo, Y. Zhang, *Immunity* **50**, 1043 (2019).
2. M. Rigau, S. Ostrouska, T. S. Fulford, D. N. Johnson, K. Woods, Z. Ruan, H. E. G. McWilliam, C. Hudson, C. Tutuka, A. K. Wheatley, S. J. Kent, J. A. Villadangos, B. Pal, C. Kurts, J. Simmonds, M. Pelzing, A. D. Nash, A. Hammet, A. M. Verhagen, G. Vairo, E. Maraskovsky, C. Panousis, N. A. Gherardin, J. Cebon, D. I. Godfrey, A. Behren, A. P. Uldrich, *Science* **367**, eaay5516 (2020).
3. L. Yuan, X. Ma, Y. Yang, Y. Qu, X. Li, X. Zhu, W. Ma, J. Duan, J. Xue, H. Yang, J.-W. Huang, S. Yi, M. Zhang, N. Cai, L. Zhang, Q. Ding, K. Lai, C. Liu, L. Zhang, X. Liu, Y. Yao, S. Zhou, X. Li, P. Shen, Q. Chang, S. R. Malwal, Y. H, W. Li, C. Chen, C.-C. Chen, E. Oldfield, R.-T. Guo, Y. Zhang, *Nature* **621**, 840 (2023).

